Time-Resolved Resonance Raman Study of the Reaction of the 2-Fluorenylnitrenium Ion with 2-Fluorenylazide

Jiadan Xue, Zhen Guo, Pik Ying Chan, Lai Man Chu, Tracy Yuen Sze But, and David Lee Phillips*

Department of Chemistry, The University of Hong Kong, Pokfulam Road, Hong Kong S.A.R., People's Republic of China

Received: October 12, 2006; In Final Form: December 5, 2006

A time-resolved resonance Raman investigation of the reaction of the 2-fluorenylnitrenium ion with 2-fluorenylazide in a mixed aqueous solvent is presented. The reaction of the 2-fluorenylnitrenium ion with 2-fluorenylazide in the mixed aqueous solution generates two new species on the microsecond time scale. One of these species is identified as 2,2′-azobisfluorene, and the other species is tentatively assigned to a 1,4-bis-(2,2′-fluorenyl)-tetrazadiene cation intermediate. The structure and properties of these two species are briefly discussed. The reaction of the 2-fluorenylnitrenium ion with 2-fluorenylazide is also briefly compared to that of the 2-fluorenylnitrenium ion reactions with guanosine and water.

I. Introduction

The photochemistry of aryl azides has been well examined, and laser flash photolysis experiments have been employed to directly investigate their reaction intermediates and photoproducts so as to increase our understanding of their reaction mechanisms.[1−60] A singlet arylnitrene species and a nitrogen molecule are typically produced from photolysis of aryl azides in room-temperature solutions. The singlet arylnitrene may then undergo very rapid ring expansion reactions to form ketenimines (dehydroazepines) that can subsequently be trapped by nucleophiles in some cases. The chemistry and reaction mechanisms of singlet phenylnitrene have been the subject of many investigations,[7,8,18,20,21,42−46,52−54] and this work found that the singlet phenylnitrene has a short lifetime of about 1 ns in room-temperature solutions because of its very fast ring expansion reaction, while the lifetimes of some substituted singlet phenylnitrenes can become substantially longer.[16−18,22−25,29,40,55,57] The longer-lived singlet arylnitrene intermediates can be trapped more easily by nucleophiles such as diethylamine or pyridine. Some of the para substituted singlet arylnitrenes can even react with water to form arylnitrenium ions.[26,28,31−37,40,47,48,61] There has been much interest in arylnitrenium ions since they are believed to play a key role in the chemical carcinogenesis of aromatic amines,[62−79] and some arylnitrenium ions have been observed to be selectively trapped by guanine bases in DNA.[69−71,75,79] Arylnitrenium ions are typically very short-lived species that are hard to directly study in room-temperature solutions, and this has led several groups to develop photochemical methods to produce arylnitrenium ions so that they can be readily studied by pump−probe spectroscopy experiments.[26,28,31−37,40,47,48,80,81] The photolysis of aryl azides to form a singlet arylnitrene that then reacts with water to produce a singlet arylnitrenium ion is one of the photochemical methods developed to make arylnitrenium ions.[26,28,31−37,40,47,48] Picosecond transient absorption[35] and time-resolved resonance Raman[82] studies observed that the 2-fluorenylnitrenium ion is formed about 100 ps after photolysis of 2-fluorenyl azide in a mixed aqueous solvent.

There are relatively few studies of direct time-resolved vibrational spectroscopic characterization of arylnitrenium ions and their reactions in room-temperature solutions. Time-resolved infrared (TRIR) has been employed to study several arylnitrenium ions in organic solvents.[48,56] We have recently reported time-resolved resonance Raman spectra for several arylnitrenium ions[61] including the first time-resolved vibrational spectra of the reaction of an arylnitrenium ion with a guanine derivative to produce a C8 intermediate.[83] In this paper, we present a time-resolved resonance Raman study of the reaction of the 2-fluorenylnitrenium ion with 2-fluorenylazide in a mixed aqueous solvent. To our knowledge, this is the first direct time-resolved vibrational spectroscopic observation of an arylnitrenium ion reaction with its corresponding aryl azide in room-temperature solutions. The reaction of the 2-fluorenylnitrenium ion with 2-fluorenylazide in the mixed aqueous solution produces two new species on the microsecond time scale. One of these species was identified as 2,2′-azobisfluorene and this was confirmed by comparison of its time-resolved resonance Raman spectrum to the resonance Raman spectrum of an authentic sample of 2,2′-azobisfluorene made from a different synthetic method. The other species was tentatively assigned to a 1,4-bis-(2,2′-fluorenyl)-tetrazadiene cation intermediate formed from addition of the 2-fluorenylnitrenium ion to the terminal nitrogen atom of 2-fluorenylazide. We briefly discuss the structure and properties of the species involved in the reaction of the 2-fluorenylnitrenium ion with 2-fluorenylazide. We also briefly compare the 2-fluorenylnitrenium ion reactions with 2-fluorenylazide to those with guanosine and water.

II. Experimental and Computational Methods

II.A. Preparation of 2-Fluorenylazide Precursor Compound and an Authentic Sample of 2,2′-Azobisfluorene. Samples of 2-fluorenylazide were synthesized according to literature methods,[84a] and further details of the synthesis and characterization are given in the Supporting Information of reference 61a. The 2-fluorenylazide samples were prepared with

* Author to whom correspondence should be addressed. Phone: 852-2859-2160. Fax: 852-2857-1586. E-mail: phillips@hkucc.hku.hk.

10.1021/jp066699y CCC: $37.00
Published on Web 02/02/2007

concentrations of ~1 mM in acetonitrile, water/acetonitrile (50:50), and water/acetonitrile (75:25) solvents for use in the TR^3 experiments. Spectroscopic grade acetonitrile and deionized water were used in preparing the sample solutions.

An authentic sample of 2,2′-azobisfluorene was prepared from 2-aminofluorene. One gram of 2-aminofluorene and 4.78 g of dried active manganese dioxide in 70 mL of benzene were refluxed using a Dean−Stark water separator for 12 h.[84c] The hot solution was filtered, and the manganese dioxide was washed with hot benzene until the filtrate was colorless. The filtrate was evaporated to a small volume and purified by column chromatography [hexane/ethyl acetate (19:1)]. The sample was characterized as follows. NMR (300 MHz), $CDCl_3$): δ 8.13 (s, 2H), 8.03 (d, 2H, J = 8.1 Hz), 7.93 (d, 2H, J = 8.1 Hz), 7.86 (d, 2H, J = 7.3 Hz), 7.59 (d, 2H, J = 7.5 Hz), 7.42 (t, 1H, J = 7.4 Hz), 7.36 (t, 1H, J = 7.4 Hz), 4.02 (s, 4H). MS (EI): m/z 358 [$C_{26}H_{18}N_2^+$], 180 [$C_{13}H_{10}N^+$], 165 [$C_{13}H_9^+$]. IR: 2961.4, 2923.5, 2847.6, 2363.3, 2328.6, 1719.9, 1604.3 cm^{-1}. Mp: 156−158 °C, deep brown solid.

II.B. Nanosecond Time-Resolved Resonance Raman (ns-TR^3) Experiments. The experimental apparatus and methods used for the ns-TR^3 experiments have been detailed elsewhere,[60,83,85] so only a brief account will be given here. The hydrogen Raman shifted laser lines for the harmonics of a Nd:YAG nanosecond pulsed laser system provided the 266 nm pump (fourth harmonic) and 368.9 nm probe (the second anti-Stokes hydrogen Raman shifted laser line of the 532 nm second harmonic) wavelengths used in the ns-TR^3 experiments. The ns-TR^3 experiments used two Nd:YAG lasers electronically synchronized to each other by a pulse delay generator employed to control the relative timing of the two lasers. A fast photodiode whose output was displayed on a 500 MHz oscilloscope was used to measure the relative timing of the pump and probe pulses with the jitter between the pump and probe pulses observed to be <5 ns. The laser beams were loosely focused onto a flowing liquid stream of sample using a near-collinear geometry, and the scattered Raman light was collected employing reflective optics and a backscattering geometry. The collected Raman light was imaged through a depolarizer mounted on the entrance of a monochromator that dispersed the light onto a liquid nitrogen cooled CCD detector that collected the Raman signal for 30−60 s before reading out to an interfaced PC computer. About 10−20 of these readouts were summed to obtain the resonance Raman spectrum. The TR^3 spectra were found by subtracting the pump−probe spectrum at negative 100 ns from the pump−probe spectra acquired at positive time delays in order to remove the solvent and precursor Raman bands. The known wavenumbers of the mixed solvent acetonitrile Raman lines were used to calibrate the wavenumbers of the TR^3 spectra to an estimated accuracy of ±5 cm^{-1}. A Lorentzian function was used to integrate the relevant Raman bands in the TR^3 spectra in order to determine their areas and to extract the decay and growth of the species observed in the experiments. During the experiments no noticeable degradation was observed for the sample by UV−vis absorption spectroscopy.

II.C. Density Functional Theory Calculations. All of the density functional theory calculations presented here made use of the Gaussian 98 program suite[86] operated on the high-performance computing cluster installed at the University of Hong Kong. Complete geometry optimization and vibrational frequency calculations were done analytically using the B3LYP method with the 6-31G* basis set for the ground states with the lowest energy configurations obtained for the 2,2′-azobisfluorene product and the 1,4-bis-(2,2′-fluorenyl)-tetrazadiene cation intermediate. A Lorentzian function with a 15 cm^{-1} bandwidth was employed with the calculated Raman vibrational frequencies and relative intensities to obtain the B3LYP/6-31G* computed Raman spectra reported in this paper.

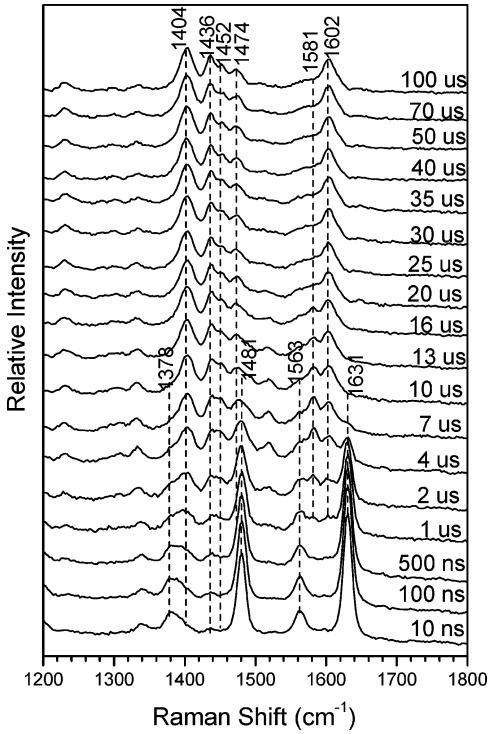

Figure 1. Overview of selected 368.9 nm probe TR^3 spectra obtained after 266 nm photolysis of 1.2 mM 2-fluorenylazide in a water/acetonitrile (50:50) mixed solvent with a 0.002 M Na_2HPO_4/0.002 M NaH_2PO_4 buffer. The time delays between the pump (266 nm) and probe (368.9 nm) laser beams are shown to the right of each spectrum, and the Raman shifts of selected bands are presented at the top of the 10 and 100 μs spectra. See text for more details.

III. Results and Discussion

III.A. Time-Resolved Resonance Raman Spectra Acquired After 266 nm Photolysis of 2-Fluorenylazide in a Water/Acetonitrile (50:50) Solution. Figures 1 and 2 display time-resolved resonance Raman (TR^3) spectra acquired at various time delays after photolysis of 1.2 mM (Figure 1) and 0.3 mM (Figure 2) 2-fluorenylazide in a water/acetonitrile (50:50), 0.002 M Na_2HPO_4/0.002 M NaH_2PO_4 buffered mixed solvent. The time delays between the pump (266 nm) and probe (368.9 nm) laser beams are shown to the right of each spectrum, and the Raman shifts of selected bands are presented at the top of the 100 μs spectrum in Figures 1 and 2. The TR^3 spectra shown in Figures 1 and 2 are similar to one another and indicate three species can be observed on over the 10 ns to 100 μs time scale. The first species has characteristic resonance Raman bands at 1378, 1481, 1563, and 1631 cm^{-1} and appears to decay to form the other two species. The second species has a characteristic Raman band at 1581 cm^{-1} (with some others overlapping with the other species Raman bands) and appears to first grow in and then decays. The third species has bands at 1404, 1436, 1452, 1474, and 1602 cm^{-1} and appears to grow in and does not decay on the 100 μs time scale. Comparison of the spectra presented in Figures 1 and 2 shows that the lifetimes of the first and second species as well as the formation rates of the second and third species are significantly different at the two different 2-fluorenylazide concentrations. This concentration-

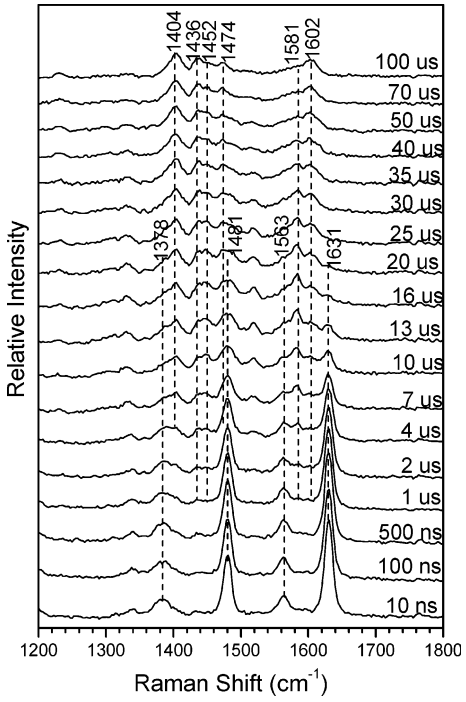

Figure 2. Overview of selected 368.9 nm probe TR^3 spectra obtained after 266 nm photolysis of 0.3 mM 2-fluorenylazide in a water/acetonitrile (50:50) mixed solvent with a 0.002 M Na_2HPO_4/0.002 M NaH_2PO_4 buffer. The time delays between the pump (266 nm) and probe (368.9 nm) laser beams are shown to the right of each spectrum, and the Raman shifts of selected bands are presented at the top of the 20 and 100 μs spectra. See text for more details.

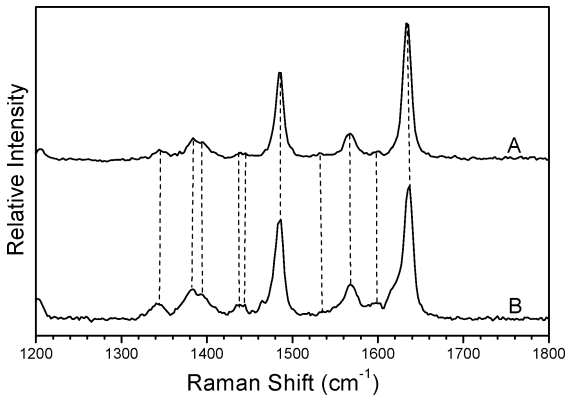

Figure 3. Comparison of (A) the 10 ns 368.9 nm probe TR^3 spectrum from Figure 1 to (B) a 10 ns 416.0 nm probe TR^3 spectrum previously reported for the 2-fluorenylnitrenium ion in reference 61b that was obtained after 266 nm photolysis of 2-fluorenylazide in a water/acetonitrile (75:25) solution. See text for more details.

dependent behavior suggests that the first species may be reacting with 2-fluorenylazide to form the other species.

Since photolysis of 2-fluorenylazide in mixed aqueous solutions has previously been observed to produce the 2-fluorenylnitrenium ion on the nanosecond time scale,[35,61a,b,82] we tentatively assign the early time species seen in Figures 1 and 2 on the nanosecond time scale (see the 10 and 100 ns spectra) to the 2-fluorenylnitrenium ion. Figure 3 shows a comparison of the 10 ns 368.9 nm probe TR^3 spectrum from Figure 1 to a 10 ns 416.0 nm probe TR^3 spectrum previously reported for the 2-fluorenylnitrenium ion in reference 61b that was obtained after 266 nm photolysis of 2-fluorenylazide in a water/acetonitrile(75:25) solution. Examination of Figure 3 shows that the two TR^3 spectra are almost identical with some modest variation in the relative intensities that can be easily attributed

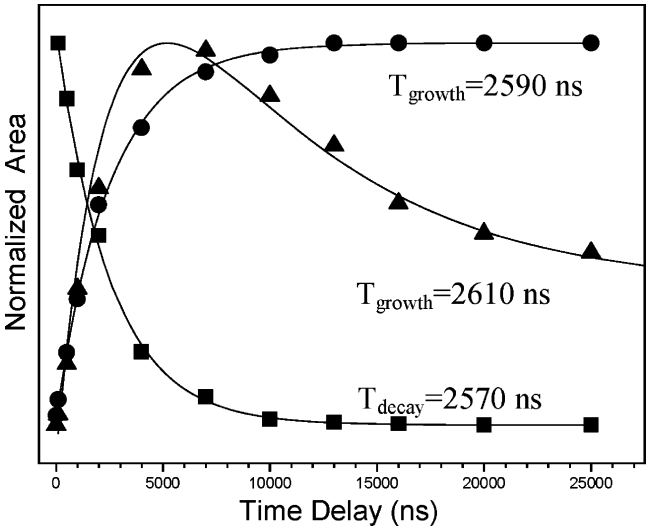

Figure 4. Plots of the integrated areas for the characteristic Raman bands for the three species observed in the TR^3 spectra of Figure 1 (the 1631 cm^{-1} band for the 2-fluorenylnitrenium ion species [solid squares], the 1581 cm^{-1} for the second species [solid triangles], and the 1602 cm^{-1} for the third species [solid circles]) as a function of time delay are shown. The data were fit to simple exponential growth and/or decay functions as shown by the curves in the figure. Each of the three kinetics curves were normalized to the largest Raman band intensity observed for each species over the 10 ns to 100 μs time scale. The time constants for the best fit exponential kinetics are indicated for the 2-fluorenylnitrenium ion decay and the second and third species growth next to the appropriate curves. See text for more details.

to the different excitation wavelengths used to generate the TR^3 spectra. This indicates the TR^3 spectra are due to the same species and confirms that the first species seen in the TR^3 spectra of Figures 1 and 2 (for example, see the 10 and 100 ns spectra) are due to the 2-fluorenylnitrenium ion. The Raman band vibrational frequencies for the 10 ns 368.9 nm TR^3 spectra of Figures 1 and 2 are compared to those previously reported for the 10 ns 416.0 nm TR^3 spectrum and density functional theory calculated frequencies from reference 61b and presented in Table S1 in the Supporting Information. This comparison is consistent with the first species observed on the nanosecond time scale in the TR^3 spectra of Figures 1 and 2 being assigned to the 2-fluorenylnitrenium ion.

III.B. Time-Dependent Behavior of Species Observed in the TR^3 Spectra. In order to examine the kinetic behavior of the three species observed in the TR^3 spectra of Figures 1 and 2, the characteristic Raman bands for the three species (1631 cm^{-1} band for the 2-fluorenylnitrenium ion species, 1581 cm^{-1} for the second species, and 1602 cm^{-1} for the third species) had their integrated areas plotted as a function of time delay in Figure 4. Each of the three kinetics curves in Figure 4 was normalized to the largest Raman band intensity observed for each species over the 10 ns to 100 μs TR^3 spectra shown in Figure 1 for the experiments done with a 1.2 mM concentration of 2-fluorenylazide. The kinetics of the 2-fluorenylnitrenium ion decay and the third species growth could be fitted satisfactorily to an exponential decay function for the 2-fluorenylnitrenium ion with a time constant of about 2570 ns and an exponential growth function for the third species with a time constant of 2590 ns (the fitted curves are shown in Figure 4). Global analysis of the integrated areas of the second species as a function of delay time indicates a combined exponential growth and exponential decay function is needed with a growth time constant of about 2610 ns (the fitted curve is shown in Figure 4). A similar kinetics analysis was done for the 0.3 mM

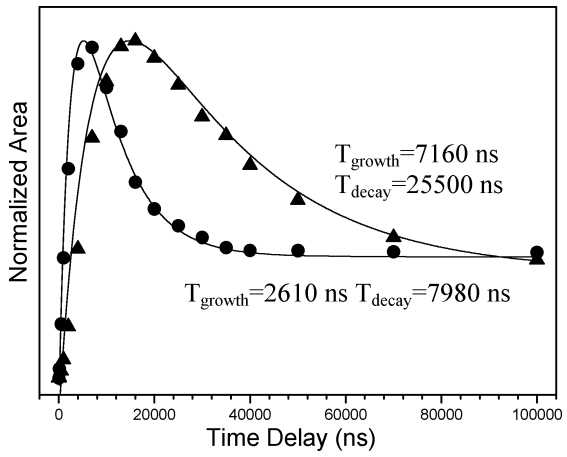

Figure 5. Kinetic analysis of the second species based on the integrated area of its 1581 cm^{-1} Raman band observed in the TR^3 spectra given in Figures 1 and 2 for the 1.2 mM (solid circles) and 0.3 mM (solid triangles) 2-fluorenylazide samples. The data were fit to an exponential growth and an exponential decay functions, and both curves shown were normalized to the maximum integrated areas observed for each sample. The time constants for the decay of the second species are indicated next to the appropriate curves. See text for more details.

2-fluorenylazide sample TR^3 spectra shown in Figure 2, and these data with the corresponding fittings are given in Figure 1S of the Supporting Information. The time constant found for the exponential decay of the 2-fluorenylnitrrenium ion was found to be about 7100 ns, and the exponential growth time constants for the second and third species were found to be about 7160 and 7140 ns, respectively, for the 0.3 mM 2-fluorenylazide sample. The time constants found for the decay of the 2-fluorenylnitrenium ion and the growth of the second and third species are all about the same and within experimental uncertainty at a given concentration. This suggests that the 2-fluorenylnitrenium ion is a precursor species for the generation of both the second and third species. This in combination with the 2-fluorenylazide concentration dependence of the 2-fluorenylnitrenium ion lifetime and the formation times of the second and third species further suggests that the 2-fluorenylnitrenium ion is reacting with 2-fluorenylazide to produce the second and third species.

Figure 5 presents a kinetic analysis of the second species based on the integrated area of its 1581 cm^{-1} Raman band for the 1.2 mM and 0.3 mM 2-fluorenylazide samples. The data were fitted to an exponential growth and an exponential decay functions, and both curves were normalized to the maximum integrated areas observed for each sample. After the second species is formed, it decays with time constants of about 7980 and 25 500 ns in the 1.2 and 0.3 mM 2-fluorenylazide sample solutions, respectively. This 2-fluorenylazide concentration dependence of the second species decay suggests that it may also be undergoing further reaction with 2-fluorenylazide. In contrast, the third species with characteristic Raman bands at 1404, 1436, 1452, 1474, and 1602 cm^{-1} does not decay over the microsecond to millisecond time scales and may be a stable product.

III.C. Assignments of Second and Third Species Observed in the TR^3 Spectra. Comparison of experimental vibrational frequencies to those predicted from density functional theory (DFT) or ab initio calculations for probable intermediates has been successfully employed to identify and assign time-resolved infrared (TRIR) and time-resolved resonance Raman (TR^3) spectra to arylnitrenium ions, arylnitrenes, and arylnitrene photoproducts.[48,56,57b,60,61a−d] We shall use a similar methodology to help assign the second and third species observed in the TR^3 spectra of Figures 1 and 2. Considering that the third species appears to be formed from reaction of the 2-fluorenylnitrenium ion with 2-fluorenylazide and has prominent resonance Raman bands in the 1400−1500 cm^{-1} region characteristic of N═N bond stretching vibrational modes, we examined the possibility that the third species is an azobenzene compound produced by the following reaction:

2-fluorenylnitrenium ion + 2-fluorenylazide → 2,2′-azobisfluorene + N_2 + H^+ (reaction 1)

B3LYP/6-31G* calculations were performed to predict the total energy, optimized geometry, and vibrational frequencies for the 2,2′-azobisfluorene species. Figure 6 compares the experimental 100 μs TR^3 spectrum from Figure 1 to the B3LYP/6-31G* calculated normal Raman spectrum whose relative intensities were convoluted with a Lorentzian function. Figure 6 shows a simple schematic diagram of the optimized geometry of the 2,2′-azobisfluorene found from the B3LYP/6-31G* calculations with selected bond lengths (in angstrom) indicated next to the appropriate bonds. Table 1 compares the experimental Raman band vibrational frequencies for the 100 μs TR^3 spectrum from Figure 1 to those predicted from the B3LYP/6-31G* calculations for 2,2′-azobisfluorene. Inspection of Table 1 reveals there is excellent agreement between the experimental and calculated vibrational frequencies with the calculated vibrational frequencies being within about 3.2 cm^{-1} on average for the 10 experimental Raman band frequencies compared to the calculated ones. Inspection of the experimental TR^3 spectrum to the calculated 2,2′-azobisfluorene spectrum also shows reasonable agreement with the calculated normal Raman spectrum of 2,2′-azobisfluorene with some moderate differences in the relative intensities that can be easily accounted for by the fact that the experimental spectrum is resonantly enhanced while the calculated spectrum is for a normal Raman spectrum. These results indicate the third species is likely the 2,2′-azobisfluorene compound. To unequivocally confirm this assignment, we made the 2,2′-azobisfluorene compound using a different synthetic method and compared its 368.9 nm resonance Raman spectrum to that of the experimental 100 μs TR^3 spectrum (from Figure 1) as shown in Figure 7. Inspection of Figure 7 shows that the two different spectra are essentially identical within experimental uncertainty, and this unambiguously confirms the assignment of the third species TR^3 spectra to the 2,2′-azobisfluorene compound. We also isolated one of the major products from 266 nm photolysis of 2-fluorenylazide in the water/acetonitrile (50:50) and obtained its 368.9 nm resonance Raman spectrum and compared it also to the TR^3 spectrum in Figure 7. This comparison in Figure 7 also clearly shows it is the same 2,2′-azobisfluorene compound and indicates that this compound is one of the major products from the photochemistry.

The second species is an intermediate and is also formed from the reaction of the 2-fluorenylnitrenium ion with 2-fluorenylazide compound and then decays on the tens of microsecond time scale. A probable reaction is an addition reaction such as the following reaction:

2-fluorenylnitrenium ion + 2-fluorenylazide → 1,4-bis-(2,2′-fluorenyl)-tetrazadiene cation (reaction 2)

In order to extract a TR^3 spectrum of the second species by itself, we employed the 7 μs TR^3 spectrum obtained in the 0.3 mM 2-fluorenylazide sample (see Figure 2) and then subtracted an appropriately scaled 2-fluorenylnitrenium ion and 2,2′-

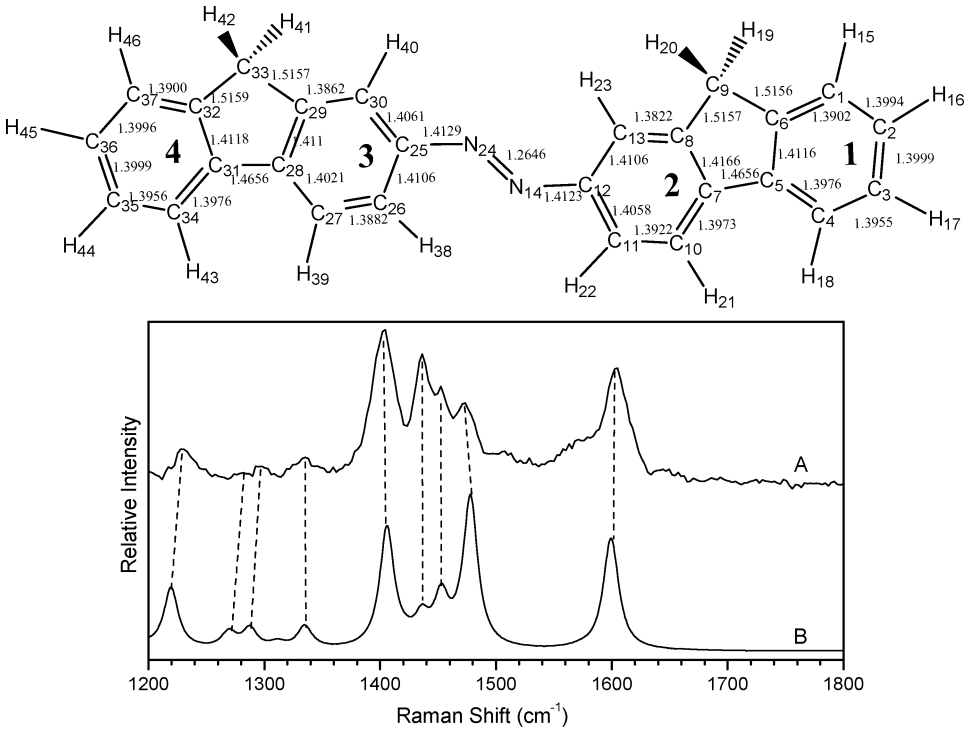

Figure 6. (Top) Simple schematic diagram of the optimized geometry of the 2,2′-azobisfluorene found from the B3LYP/6-31G* calculations with selected bond lengths (in angstrom) indicated next to the appropriate bonds. (Bottom) Comparison of (A) the experimental 100 μs TR^3 spectrum from Figure 1 to (B) the B3LYP/6-31G* calculated normal Raman spectrum whose relative intensities were convoluted with a Lorentzian function. See text and Table 1 for more details.

TABLE 1: Comparison of the B3LYP/6-31G* Calculated Raman Vibrational Frequencies for the 2,2′-Azobisfluorene Compound to Those Observed for the 100 μs TR^3 Experimental Spectrum of Figure 1[a]

	vibrational mode possible description	**calculated** B3LYP/6-31G* calcd (cm^{-1})	**experiment** Raman frequency shift (in cm^{-1})
ν_{87}	**C−H bend + C−C stretch (all) + C−N stretch**	**1220**	**1228**
ν_{88}	CH_2 bend + C−H bend + C−N stretch	1243	
ν_{89}	CH_2 bend + C−H bend	1267	
ν_{90}	**CH_2 bend + C−H bend + C5−C7 stretch**	**1270**	**1276**
ν_{91}	CH_2 bend + C−H bend (ring 1 major) + C−C stretch (ring 2 major)	1287	
ν_{92}	**CH_2 bend + C−H bend (ring 4 major) + C−C stretch (ring 3 major)**	**1288**	**1295**
ν_{93}	C−C stretch (all)	1310	
ν_{94}	CH_2 bend + C−C stretch (all)	1314	
ν_{95}	**CH_2 scissor + C−C stretch (ring 3, 4 major)**	**1335**	**1335**
ν_{96}	C−C stretch (ring 2) + N═N stretch	1342	
ν_{97}	**C−C stretch (ring 3) + N═N stretch**	**1406**	**1404**
ν_{98}	CH_2 scissor + C−C stretch (ring 3 major)	1417	
ν_{99}	$C33H_2$ scissor	1423	
ν_{100}	$C9H_2$ scissor	1423	
ν_{101}	**CH_2 scissor + C−H bend + C−C stretch (ring 1, 2 major) + N═N stretch**	**1436**	**1436**
ν_{102}	C−H bend + C−C stretch (all)	1444	
ν_{103}	**CH_2 scissor + C−H bend + C−C stretch (ring 3, 4 major) + N═N stretch**	**1453**	**1452**
ν_{104}	CH_2 scissor + C−C stretch (ring 1 major)	1457	
ν_{105}	CH_2 scissor + C−C stretch (ring 1, 2 major)	1465	
ν_{106}	**$C9H_2$ scissor + C−C stretch (all) + N═N stretch**	**1469**	**1474**
ν_{107}	C−C stretch (all) + N═N stretch	1478	
ν_{108}	C−C stretch (ring 3 major) + N═N stretch	1556	
ν_{109}	C−C stretch (ring 2 major) + N═N stretch	1566	
ν_{110}	C−C stretch (ring 1)	1574	
ν_{111}	**C−C stretch (ring 4)**	**1574**	**1571**
ν_{112}	C−C stretch (all) + N═N stretch	1596	
ν_{113}	C−C stretch (all) + N═N stretch	1599	
ν_{114}	C−C stretch (all)	1600	
ν_{115}	**C−C stretch (all) + N═N stretch**	**1602**	**1602**

[a] Experimental vibrational frequencies are compared to those from B3LYP/6-31G* computations for the 2,2′-azobisfluorene compound. See the text for more details. Possible vibrational band assignments are also shown based on comparison to the calculated vibrational frequencies from the B3LYP/6-31G* computations in the 1200−1600 cm^{-1} fingerprint region for the 2,2′-azobisfluorene compound.

azobisfluorene TR^3 spectra. Figure 8 displays the experimental TR^3 spectrum derived for the second species at 7 μs and compares it to the normal Raman spectra calculated for two isomers of the 1,4-bis-(2,2′-fluorenyl)-tetrazadiene cation in-

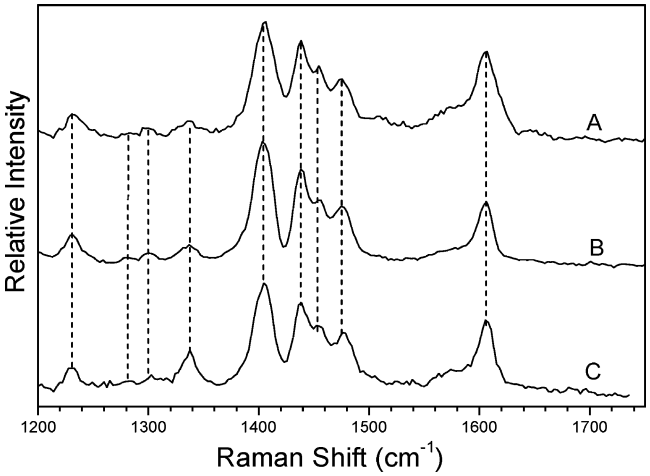

Figure 7. Comparison of the experimental 100 μs TR^3 spectrum (A) from Figure 1 to the 368.9 nm resonance Raman spectrum of an authentic sample of 2,2′-azobisfluorene compound (B) made using a different synthetic method. These spectra are also compared to the 368.9 nm resonance Raman spectrum of one of the isolated major products (C) obtained from the 266 nm photolysis of 2-fluorenylazide in the water/acetonitrile (50:50) solution. This comparison clearly shows that the third species observed in the TR^3 spectra of Figures 1 and 2 is the 2,2′-azobisfluorene compound and that this compound is one of the major products from the photochemistry. See text for more details.

termediates from B3LYP/6-31G* computations. Table 2 compares the TR^3 vibrational frequencies for the second species to those obtained from the B3LYP/6-31G* calculations for the 1,4-bis-(2,2′-fluorenyl)-tetrazadiene cation intermediates. Examination of Table 2 shows there is excellent agreement between the experimental and calculated vibrational frequencies with the calculated vibrational frequencies being within about 3.1 and 3.5 cm^{-1} for isomer A and isomer B, respectively, on average for the 13 experimental Raman band frequencies compared to the calculated ones. Comparison of the experimental TR^3 spectrum to the calculated 1,4-bis-(2,2′-fluorenyl)-tetrazadiene cation isomers spectra in Figure 8 also exhibits reasonable agreement with the calculated normal Raman spectra of 1,4-bis-(2,2′-fluorenyl)-tetrazadiene cations considering the fact that the experimental spectrum is resonantly enhanced while the calculated spectra are for normal Raman spectra which make their relative intensity patterns somewhat different. These results indicate the second species are likely 1,4-bis-(2,2′-fluorenyl)-tetrazadiene cation intermediates.

The neutral forms (free base) of the tetrazadiene species were also considered as a possibility when identifying the second species observed in our experiments. The predicted Raman spectra of the tetrazadiene neutral forms appear somewhat similar to those of the 1,4-bis-(2,2′-fluorenyl)-tetrazadiene cation intermediates and that of the second species obtained from experiment (the calculated tetrazadiene neutral forms spectra and details are displayed in Figure 2S of the Supporting Information). But, the calculated Raman spectra for the neutral forms (free base) of the tetrazadiene species do not agree as well with the second species experimental TR^3 spectra as those of the 1,4-bis-(2,2′-fluorenyl)-tetrazadiene cation intermediates, and we still assign the second species to the tetrazadiene cation rather than its neutral form. If the second species were the tetrazadiene neutral form, its decay process observed during the experiment would likely be related to a deprotonation, and a tetrazadiene species would be formed, in which no hydrogen is attached to nitrogen atom. On the basis of results from TD DFT calculations, the tetrazadiene species can be observed with the 368.9 nm probe wavelength used in experiments. However, no new species was observed at longer delay times in the TR^3 experiments except the 2,2-azobisfluorene product and there was no evidence for appreciable formation of tetrazadiene. While the second species decays, the intensity of the Raman bands belonging to the 2,2-azobisfluorene product did not increase in intensity (the Raman bands of tetrazadiene and 2,2-azobisfluorene overlap to some extent based on the results from the calculations), and this is consistent with little or no appreciable formation of tetrazadiene. The final products were separated and analyzed using mass spectroscopy, and no characteristic peaks of tetrazadiene were observed. These computational and experimental results suggest that no appreciable tetrazadiene species was formed under the experimental conditions examined here. Therefore, we excluded the assignment of the second species to a tetrazadiene neutral intermediate and assigned the second species to a 1,4-bis-(2,2′-fluorenyl)-tetrazadiene cation intermediate.

III.D. Discussion of the 2-Fluorenylnitrenium Ion Reactions with 2-Fluorenylazide. The first species observed in the TR^3 spectra shown in Figures 1 and 2 has been identified as the 2-fluorenylnitrenium ion which is presumably formed from the fast reaction of the singlet 2-fluorenylnitrene species with water as previously observed in picosecond transient absorption and TR^3 experiments.[35,82] Previous transient absorption quenching experiments determined that the 2-fluorenylnitrenium ion reacts with the azide anion (N_3^-) and water with rate constants of about 5×10^9 M^{-1} s^{-1} and 3×10^4 s^{-1}, respectively.[87] In addition, time-resolved transient absorption and TR^3 experiments indicated that the 2-fluorenylnitrenium ion reacts with guanosine with a rate constant of about 7.6×10^8 M^{-1} s^{-1} to form a C8 intermediate species.[80,83] In the absence of an azide anion, guanosine (or other guanine derivatives) or other similar species, the 2-fluorenylnitrenium ion will likely be quenched by either water or any remaining unphotolyzed 2-fluorenylazide precursor in a largely water containing solution. Our results here indicate that the 2-fluorenylnitrenium ion can react with the 2-fluorenylazide compound with a rate constant on the order of 3×10^8 M^{-1} s^{-1} and quenching of the 2-fluorenylnitrenium ion occurs predominantly by reaction with the remaining 2-fluorenylazide at the concentrations examined here. The rate constant for reaction of the 2-fluorenylnitrenium ion with 2-fluorenylazide is substantially faster than that for the 2-fluorenylnitrenium ion with water (3×10^4 s^{-1}) and is somewhat slower than that for the 2-fluorenylnitrenium ion with guanosine (about 7.6×10^8 M^{-1} s^{-1}) to form a C8 intermediate species.[80,83] Thus, guanosine or other guanine derivatives can compete with quenching of the 2-fluorenylnitrenium ion by the parent 2-fluorenylazide species when the guanosine (or other guanine derivatives) have concentrations similar to or greater than the concentration of the remaining unphotolyzed 2-fluorenylazide.

It is interesting to note that for both thermal and photoinduced decompositions of aryl azides, it was suggested that the arylnitrene (ArN) reacts at N_α of the azide (ArN_3) to make the azo product (Ar−N=N−Ar) and at N_γ to yield a 1,4-diaryltetrazadiene (Ar−N=N−N=N−Ar) as an unobserved reactive intermediate[1a] as shown in reactions 3 and 4 below:

$$ArN + ArN_3 \rightarrow Ar{-}N{=}N{-}Ar + N_2 \quad \text{(reaction 3)}$$

$$ArN + ArN_3 \rightarrow Ar{-}N{=}N{-}N{=}N{-}Ar \quad \text{(reaction 4)}$$

McDonald and Chowdhury[88] studied the reaction of the phenylnitrene anion radical ($PhN^{-\bullet}$) with phenylazide (PhN_3) using mass spectrometry experiments and observed the formation of

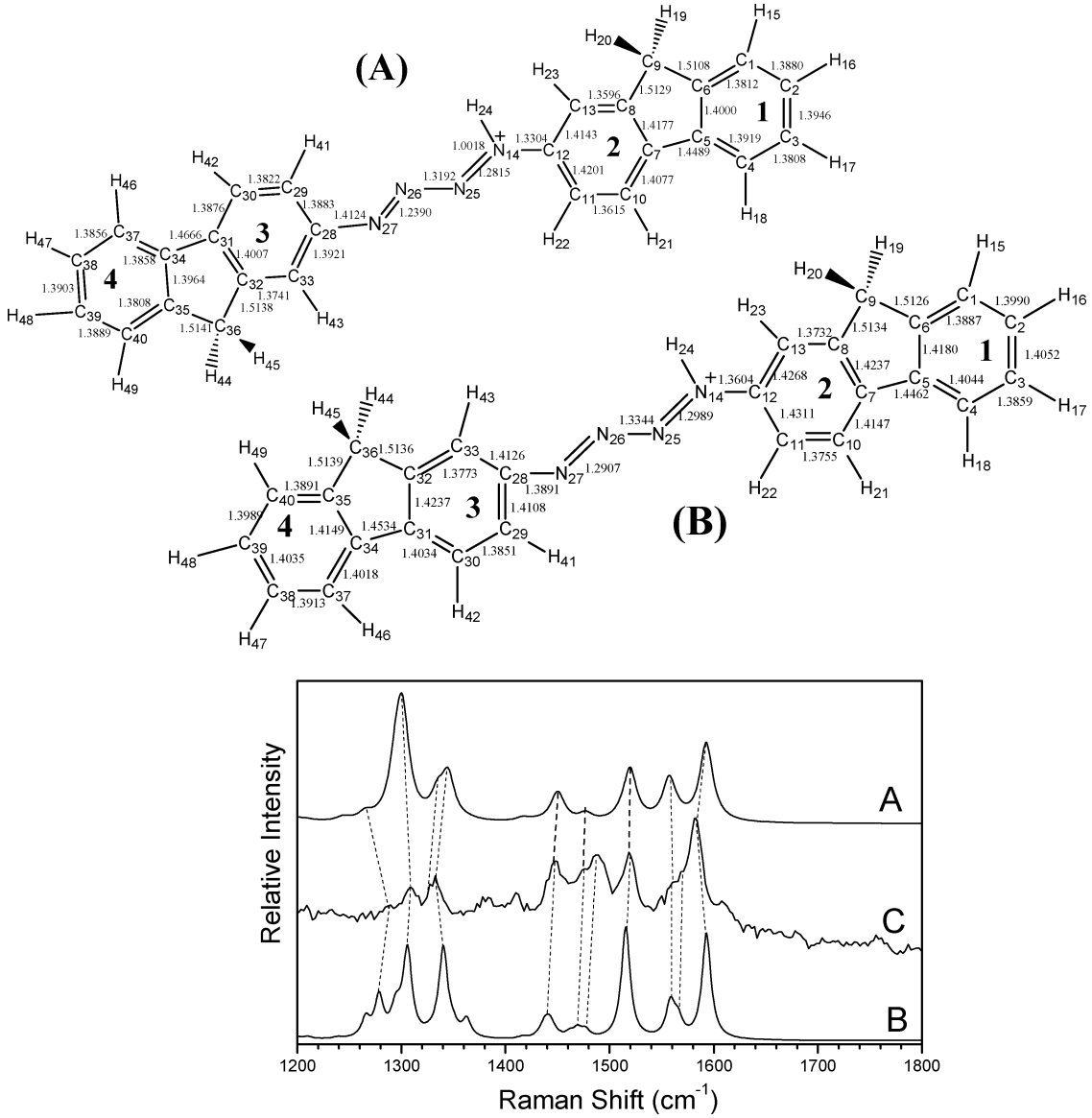

Figure 8. (Top A, B) Simple schematic diagrams of the optimized geometry of two isomers of the 1,4-bis-(2,2′-fluorenyl)-tetrazadiene cation intermediates found from the B3LYP/6-31G* calculations with selected bond lengths (in angstrom) indicated next to the appropriate bonds. (Bottom) Comparison of (C) the experimental TR^3 spectrum derived for the second species by itself from the 7 μs spectrum to (A, B) the normal Raman spectrum calculated for two isomers of the 1,4-bis-(2,2′-fluorenyl)-tetrazadiene cation intermediates from B3LYP/6-31G* computations (spectra A and B correspond to structures A and B, respectively). See text and Table 2 for more details.

two new higher mass species corresponding to Ph−N═N−Ph$^{-\bullet}$ (*m*/*z* 182) and Ph−N═N−N═N−Ph$^{-\bullet}$ (*m*/*z* 210) species. The ratio of these two signals was 1:4, and the rate constant and branching ratio were both independent of the flow velocity and flow pressure, which suggested that both product ions were formed in primary reaction channels.[88] Two possible reactions consistent with the mass spectrometry results could be the following reactions 5 and 6:

$$PhN^{-\bullet} + PhN_3 \rightarrow Ph{-}N{=}N{-}Ph^{-\bullet} + N_2 \quad \text{(reaction 5)}$$

$$PhN^{-\bullet} + PhN_3 \rightarrow Ph{-}N{=}N{-}N{=}N{-}Ph^{-\bullet} \quad \text{(reaction 6)}$$

We note that reactions 5 and 6 are similar to both reactions 3 and 4 as well as reactions 1 and 2 studied here in that reactions 1, 3, and 5 all appear to add to the N_α bond of the azide to form the corresponding azo product with the elimination of a N_2 byproduct while reactions 2, 4, and 6 all add to the azide to form the corresponding 1,4-diaryltetrazadiene species. Our present results indicate the 2-fluorenylnitrenium ion undergoes similar addition reactions which either form a stable azo product (2,2′-azobisfluorene) with elimination of a N_2 byproduct or produce a 1,4-bis-(2,2′-fluorenyl)-tetrazadiene cation intermediate. An interesting difference between the 2-fluorenylnitrenium ion + 2-fluorenylazide → 2,2′-azobisfluorene + N_2 + H^+ reaction 1 and reactions 3 and 5 is the additional cleavage of the N−H^+ bond to form a H^+ by product. Since this reaction was observed here in a largely aqueous solution, this may be a water-assisted cleavage in which the explicit hydrogen bonding and solvation of the ion by the water molecules helps make the overall reaction 1 very fast. It is possible that reaction 1 could be a two-step process where the first step is the corresponding cation reaction ($ArNH^+ + ArN_3 \rightarrow [Ar{-}N(H){=}N{-}Ar]^+ + N_2$) of the analogous anion reaction 5 that is followed by a fast water-assisted cleavage of the N−H^+ bond in the [Ar−N(H)═N−Ar]$^+$ species. At this point it is not clear if the 2-fluorenylnitrenium ion + 2-fluorenylazide → 2,2′-azobisfluorene + N_2 + H^+ reaction 1 is a concerted or sequential process.

TABLE 2: Comparison of the B3LYP/6-31G* Calculated Raman Vibrational Frequencies for Two Isomers of the 1,4-Bis-(2,2′-fluorenyl)-tetrazadiene Cation Intermediates to Those Observed for the Experimental TR³ Spectrum Derived for the Second Species by Itself from the 7 μs Spectrum of Figure 2 (See the Text for Details for How This Spectrum Was Extracted)[a]

isomer A of tetrazadiene cation			isomer B of tetrazadiene cation			
	vibrational mode possible description	B3LYP/6-31G* calcd (cm^{-1})		vibrational mode possible description	B3LYP/6-31G* calcd (cm^{-1})	exptl
ν_{91}	C−H bend + N−H bend	1211	ν_{91}	C−H bend + N−H bend	1210	
ν_{92}	C−H bend (ring 1, 2) + N−H bend + C−N stretch	1244	ν_{92}	C−H bend (ring 1, 2) + N−H bend + C−N stretch	1239	
ν_{93}	C−H bend (ring 2, 3, 4) + CH_2 bend + N−H bend + N26−N27 stretch	1266	ν_{93}	C−H bend (ring 2, 3, 4) + CH_2 bend + N−H bend + N26−N27 stretch	1266	
ν_{94}	**C−H bend + CH_2 bend**	**1287**	ν_{94}	C−H bend (ring 2) + CH_2 bend	1279	**1287**
ν_{95}	C−H bend + N−H bend + C31−C34 stretch + C28−N27 stretch + N14−N25 stretch	1294	ν_{95}	**C−H bend + N−H bend + C31−C34 stretch + C28−N27 stretch + N14−N25 stretch**	**1292**	
ν_{96}	C−H bend (ring 1, 2) + CH_2 bend + N−H bend	1295	ν_{96}	C−H bend (ring 1, 2) + CH_2 bend + N−H bend + C5−C7 stretch	1295	
ν_{97}	C−H bend + CH_2 bend + N−H bend + C−C stretch + N26−N27 stretch	1300	ν_{97}	C−H bend (ring 3, 4) + CH_2 bend + N−H bend + C−C stretch (ring 3) + N26−N27 stretch	1301	
ν_{98}	**C−H bend (ring 3, 4) + CH_2 bend + N−H bend + C−C stretch + C−N stretch**	**1302**	ν_{98}	**C−H bend (ring 1, 2) + C−C stretch + C−N stretch**	**1306**	**1308**
ν_{99}	**CH_2 bend + C−C stretch**	**1327**	ν_{99}	**CH_2 bend + C−C stretch (ring 1, 2 major)**	**1327**	**1327**
ν_{100}	**CH_2 bend + C−C stretch + N14−N25 stretch**	**1335**	ν_{100}	**CH_2 bend + C−C stretch (ring1, 3, 4) + N14−N25 stretch**	**1335**	**1332**
ν_{101}	C−H bend + N−H bend + C−C stretch + C28−N27 stretch + N14−N25 stretch	1345	ν_{101}	C−H bend (ring 2, 3) + N−H bend + C−C stretch + C28−N27 stretch + N14−N25 stretch	1340	
ν_{102}	N−H bend + C−C stretch + N26−N27 stretch + N14−N25 stretch	1346	ν_{102}	N−H bend + C−C stretch + C28−N27 stretch + N14−N25 stretch	1350	
ν_{103}	C−C stretch	1365	ν_{103}	C−C stretch + N26−N27 stretch	1363	
ν_{104}	**CH_2 scissor**	**1413**	ν_{104}	**$C36H_2$ scissor**	**1415**	**1409**
ν_{105}	CH_2 scissor	1416	ν_{105}	$C9H_2$ scissor	1418	
ν_{106}	C−H bend + C−C stretch (ring 1, 2) + C28−N27 stretch + N26−N27 stretch	1426	ν_{106}	C−H bend + C−C stretch (ring 3, 4) + C28−N27 stretch + N26−N27 stretch	1432	
ν_{107}	C−H bend (ring 3, 4) + N−H bend + C−C stretch (ring 3, 4) + C28−N27 stretch	1435	ν_{107}	C−H bend (ring 1, 2) + N−H bend + C−C stretch (ring 1, 2) + C28−N27 stretch	1438	
ν_{108}	**C−H bend (ring 1, 2) + C−C stretch**	**1444**	ν_{108}	**C−H bend (ring 1, 2 major) + C−C stretch (ring 1, 2) + N14−C12 stretch**	**1442**	**1440**
ν_{109}	**$C36H_2$ scissor + C−C stretch**	**1445**	ν_{109}	**$C36H_2$ scissor + C−C stretch (ring 3, 4)**	**1446**	**1447**
ν_{110}	$C9H_2$ scissor + C−C stretch (ring 1, 2)	1450	ν_{110}	$C36H_2$ scissor + C−C stretch (ring 3, 4)	1452	
ν_{111}	CH_2 scissor + C−C stretch	1453	ν_{111}	$C9H_2$ scissor + N−H bend + C−C stretch (ring 1, 2) + N14−C12 stretch	1462	
ν_{112}	**$C9H_2$ scissor + C−H bend + C−C stretch (ring** 1, 2) + N14−C12 stretch	**1475**	ν_{112}	**$C9H_2$ scissor + N−H bend + C−C stretch (ring 1, 2) + N14−C12 stretch**	**1469**	**1474**
ν_{113}	**$C36H_2$ scissor + C−C stretch (ring 3, 4) + C28−N27 stretch**	**1477**	ν_{113}	**$C36H_2$ scissor + C−C stretch (ring 3, 4) + C28−N27 stretch**	**1477**	**1486**
ν_{114}	C−C stretch (ring 3, 4)	1512	ν_{114}	CC stretch (ring 3, 4)	1511	
ν_{115}	**N−H bend + C−C stretch (ring 2) + N26−N27 stretch + N14−C12 stretch**	**1520**	ν_{115}	**N−H bend + C−C stretch (ring 2) + N26−N27 stretch + N24−N25 stretch + N14−C12 stretch**	**1516**	**1518**
ν_{116}	N−H bend + C−C stretch (ring 1, 2) + N14−N25 stretch	1557	ν_{116}	N−H bend + C−C stretch (ring 1, 2) + N14−N25 stretch	1558	
ν_{117}	**C−C stretch (ring 4)**	**1561**	ν_{117}	**C−C stretch (ring 4)**	**1561**	**1560**
ν_{118}	N−H bend + C−C stretch (ring 1)	1567	ν_{118}	N−H bend + C−C stretch (ring 1, 2)	1566	
ν_{119}	**C−C stretch (all, symmetric) + N−H bend + N26−N27 stretch + N14−N25 stretch**	**1588**	ν_{119}	**C−C stretch (all, symmetric) + N−H bend + N26−N27 stretch + N14−N25 stretch**	**1588**	**1583**
ν_{120}	C−C stretch (ring 1, 2, 4) + N−H bend + N26−N27 stretch + N14−N25 stretch	1593	ν_{120}	C−C stretch (ring 1, 2, 4) + N−H bend + N26−N27 stretch + N14−N25 stretch	1593	
ν_{121}	C−C stretch (all) + N−H bend + N26−N27 stretch + N14−N25 stretch	1598	ν_{121}	C−C stretch (all) + N−H bend + N26−N27 stretch + N14−N25 stretch	1597	
ν_{122}	**C−C stretch (ring 2, 3, 4) + N−H bend + N26−N27 stretch + N14−N25 stretch**	**1604**	ν_{122}	**C−C stretch (ring 2, 3, 4) + N−H bend + N26−N27 stretch + N14−N25 stretch**	**1603**	**1607**

[a] Possible vibrational band assignments are also shown based on comparison to calculated vibrational frequencies from B3LYP/6-31G* computations in the 1200−1600 cm^{-1} fingerprint region for two isomers of the 1,4-bis-(2,2′-fluorenyl)-tetrazadiene cation intermediates.

It is interesting to compare some of the structural features of the 2-fluorenylnitrenium ion, the 2,2′-azobisfluorene product, and the 1,4-bis-(2,2′-fluorenyl)-tetrazadiene cation intermediate observed in the TR^3 spectra reported here. The 2-fluorenylnitrenium ion has significant iminocyclohexadienyl character with a C12−N14 bond length of about 1.2924 Å and C−C bond alternation of about 1.4710 Å for C11−C12, 1.3586 Å for C10−C11, 1.4671 Å for C12−C13, and 1.3560 Å for C8−C13 in the phenyl ring the C−N bond is attached (the numbering of the atoms follows that given in the Supporting Information for the 2-fluorenylnitrenium ion). There is still some iminocyclohexadienyl character in the 1,4-bis-(2,2′-fluorenyl)-tetrazadiene cation intermediate, but it is noticeably less than that for the 2-fluorenylnitrenium ion. For example, the C12−N14 and C28−N27 bond lengths were calculated to be 1.3604 and 1.3891 Å, respectively, compared to the 1.2924 Å for the C12−N14 bond length of the 2-fluorenylnitrenium ion. Similarly, the C−C bond alternation (or cyclohexadienyl character) is less for the 1,4-bis-(2,2′-fluorenyl)-tetrazadiene cation compared to that of the 2-fluorenylnitrenium ion. For example, the C−C bond alternation is about 1.4268 Å for C12−C13, 1.3732 Å for C13−C8, 1.4311 Å for C12−C11, and 1.3755 Å for C11−C10 in the phenyl ring the C12−N14 bond is attached in the 1,4-bis-(2,2′-fluorenyl)-tetrazadiene cation compared to the corresponding C−C bond alternation of about 1.4710 Å for C11−C12, 1.3586 Å for C10−C11, 1.4671 Å for C12−C13, and 1.3560 Å for C8−C13 in the phenyl ring the C−N bond is attached in the 2-fluorenylnitrenium ion. In contrast, the 2,2′-azobisfluorene product has little iminocyclohexadienyl character with C−N bond lengths of about 1.4123 and 1.4129 Å that are substantially longer than in the two cation species and much smaller C−C bond alternation in the phenyl rings (for example, the C−C bond alternation is about 1.4106 Å for C12−C13, 1.3822 Å for C13−C8, 1.4058 Å for C11−C12, and 1.3922 Å for C10−C11 in the phenyl ring the C12−N14 bond is attached in the 2,2′-azobisfluorene product).

It is interesting to note that the 1,4-bis-(2,2′-fluorenyl)-tetrazadiene cation decays faster at a higher concentration of the 2-fluorenylazide compound that suggests this intermediate may be further reacting with the 2-fluorenylazide compound. Since the 1,4-bis-(2,2′-fluorenyl)-tetrazadiene cation has a similar iminocyclohexadienyl character (and possibly similar chemical reactivity) as the 2-fluorenylnitrenium ion that undergoes reaction with the 2-fluorenylazide compound to make either the 2,2′-azobisfluorene product or the 1,4-bis-(2,2′-fluorenyl)-tetrazadiene cation intermediate, it is reasonable to suggest that the 1,4-bis-(2,2′-fluorenyl)-tetrazadiene cation intermediate can also undergo analogous reactions with 2-fluorenylazide to produce larger oligomeric species. This can account for the apparent reaction of the 1,4-bis-(2,2′-fluorenyl)-tetrazadiene cation intermediate with the 2-fluorenylazide compound and is consistent with the similar structural properties of the 1,4-bis-(2,2′-fluorenyl)-tetrazadiene cation intermediate with the 2-fluorenylnitrenium ion. We also note that some arylnitrenium ions like the diphenylnitrenium ion were found to produce some oligomers from nontrapping photolysis,[89] and this may be somewhat similar to the reactions we observe for the 2-fluorenylnitrenium ion and the 1,4-bis-(2,2′-fluorenyl)-tetrazadiene cation intermediate with 2-fluorenylazide to make larger species. This suggests that further work on the chemical reactivity of the 1,4-bis-(2,2′-fluorenyl)-tetrazadiene cation intermediate and related species in other arylnitrenium ion reactions with arylazides to make larger oligomeric materials may yield interesting results and help to better understand the chemistry of 1,4-diaryltetrazadiene cation intermediates.

IV. Conclusions

A time-resolved resonance Raman study of the reaction of the 2-fluorenylnitrenium ion with 2-fluorenylazide in a mixed aqueous solvent is reported. The reaction of the 2-fluorenylnitrenium ion with 2-fluorenylazide in the mixed aqueous solution produces two new species on the microsecond time scale with one identified as 2,2′-azobisfluorene and the other species tentatively assigned to a 1,4-bis-(2,2′-fluorenyl)-tetrazadiene cation intermediate. The reaction of the 2-fluorenylnitrenium ion with the 2-fluorenylazide compound was determined to have a rate constant on the order of 3×10^8 M^{-1} s^{-1}, and this is somewhat slower than that for the 2-fluorenylnitrenium ion with guanosine (about 7.6×10^8 M^{-1} s^{-1}) to form a C8 intermediate species.[80,83] At the concentrations used in our experiments, the quenching of the 2-fluorenylnitrenium ion occurs mainly by reaction with the remaining 2-fluorenylazide. We briefly discuss the structure and properties of the species involved in the reaction of the 2-fluorenylnitrenium ion with 2-fluorenylazide. The 1,4-bis-(2,2′-fluorenyl)-tetrazadiene cation intermediate has significant iminocyclohexadienyl character, but the degree is noticeably less than that for the 2-fluorenylnitrenium ion. The 2,2′-azobisfluorene product on the other hand has little iminocyclohexadienyl character. The 1,4-bis-(2,2′-fluorenyl)-tetrazadiene cation intermediate decayed faster at a higher concentration of the 2-fluorenylazide compound, which suggests it may further react with the 2-fluorenylazide compound in a manner similar to the 2-fluorenylnitrenium ion reaction with 2-fluorenylazide. The similar quenching of the 2-fluorenylnitrenium ion and the 1,4-bis-(2,2′-fluorenyl)-tetrazadiene cation intermediate by 2-fluorenyl azide appears correlated with the similar iminocyclohexadienyl character (and possibly similar chemical reactivity) of the 2-fluorenylnitrenium ion and 1,4-bis-(2,2′-fluorenyl)-tetrazadiene cation intermediate species.

Acknowledgment. This work was supported by Grants from the Research Grants Council (RGC) of Hong Kong (HKU 7040/06P) to D.L.P.

Supporting Information Available: Comparison of the Raman band vibrational frequencies for the 10 ns 368.9 nm TR^3 spectra of Figures 1 and 2 to those previously reported for the 10 ns 416.0 nm TR^3 spectrum and density functional theory calculated frequencies from reference 61b (Table S1); the integrated areas of the second species as a function of delay time done for the 0.3 mM 2-fluorenylazide sample TR^3 spectra shown in Figure 2 and fits to the data by a combined exponential growth and exponential decay function (Figure 1S); simple schematic diagrams of the optimized geometry of two isomers of the 1,4-bis-(2,2′-fluorenyl)-tetrazadiene neutral intermediates found from the UB3LYP/6-31G* calculations and comparison of the experimental TR^3 spectrum of the second species to the normal Raman spectra calculated for the 1,4-bis-(2,2′-fluorenyl)-tetrazadiene neutral intermediates (Figure 2S); simple schematic diagram of the optimized geometry obtained from B3LYP/6-31G* calculations with the atoms numbered and selected bond lengths indicated for the 2-fluorenylnitrenium ion (Figure 3S); Cartesian coordinates, total energies, and vibrational zero-point energies for the optimized geometry from the B3LYP/6-31G* calculations for the 2-fluorenylnitrenium ion, 2,2′-azobisfluorene product, two isomers of the 1,4-bis-(2,2′-fluorenyl)-tetrazadiene cation intermediates, and two isomers of the 1,4-bis-(2,2′-

fluorenyl)-tetrazadiene neutral intermediates. This material is available free of charge via the Internet at http://pubs.acs.org.

References and Notes

(1) (a) Smith, P. A. S. In *Nitrenes*; Lwowski, W., Ed.; Wiley-Interscience: New York, 1970; Chapter 4. (b) Scriven, E. F. V. In *Reactive Intermediates*; Abramovich, R. A., Ed.; Plenum: New York, 1982; Vol. 2, Chapter 1.

(2) Wentrup, C. C. *Reactive Molecules*; Wiley-Interscience: New York, 1984; Chapter 4.

(3) Platz, M. S. In *Azides and Nitrenes: Reactivity and Utility*; Scriven, E. F. V., Ed.; Academic: New York, 1984; Chapter 7.

(4) Platz, M. S.; Maloney, V. M. In *Kinetics and Spectroscopy of Carbenes and Biradicals*; Platz, M. S., Ed.; Plenum: New York, 1990; pp 303−320.

(5) Platz, M. S.; Leyva, E.; Haider, K. *Org. Photochem.* **1991**, *11*, 367−398.

(6) Schuster, G. B.; Platz, M. S. *Adv. Photochem.* **1992**, *17*, 69−143.

(7) Platz, M. S. *Acc. Chem. Res.* **1995**, *28*, 487−492.

(8) Borden, W. T.; Gritsan, N. P.; Hadad, C. M.; Karney, W. L.; Kemnitz, C. R.; Platz, M. S. *Acc. Chem. Res.* **2000**, *33*, 765−771.

(9) Schrock, A. K.; Schuster, G. B. *J. Am. Chem. Soc.* **1984**, *106*, 5228−5234.

(10) Donnelly, T.; Dunkin, I. R.; Norwood, D. S. D.; Prentice, A.; Shields, C. J.; Thomson, P. C. P. *J. Chem. Soc., Perkin Trans.* **1985**, *2*, 307−310.

(11) Dunkin, I. R.; Donnelly, T.; Lockhart, T. S. *Tetrahedron Lett.* **1985**, *26*, 359−362.

(12) Leyva, E.; Platz, M. S. *Tetrahedron Lett.* **1985**, *26*, 2147−2150.

(13) Leyva, E.; Platz, M. S.; Persy, G.; Wirz, J. *J. Am. Chem. Soc.* **1986**, *108*, 3783−3790.

(14) Shields, C. J.; Chrisope, D. R.; Schuster, G. B.; Dixon, A. J.; Poliakoff, M.; Turner, J. J. *J. Am. Chem. Soc.* **1987**, *109*, 4723−4726.

(15) Li, Y.-Z.; Kirby, J. P.; George, M. W.; Poliakoff, M.; Schuster, G. B. *J. Am. Chem. Soc.* **1988**, *110*, 8092−8098.

(16) Poe, R.; Grayzar, J.; Young, M. J. T.; Leyva, E.; Schnapp, K.; Platz, M. S. *J. Am. Chem. Soc.* **1991**, *113*, 3209−3211.

(17) Young, M. J. T.; Platz, M. S. *J. Org. Chem.* **1991**, *56*, 6403−6406.

(18) Poe, R.; Schnapp, K.; Young, M. J. T.; Grayzar, J.; Platz, M. S. *J. Am. Chem. Soc.* **1992**, *114*, 5054−5067.

(19) Younger, C. G.; Bell, R. A. *J. Chem. Soc., Chem. Commun.* **1992**, 1359−1361.

(20) Kim, S.-J.; Hamilton, T. P.; Schaefer, H. F. *J. Am. Chem. Soc.* **1992**, *114*, 5349−5355.

(21) Hrovat, D. A.; Waali, E. E.; Borden, W. T. *J. Am. Chem. Soc.* **1992**, *114*, 8698−8699.

(22) Marcinek, A.; Platz, M. S. *J. Phys. Chem.* **1993**, *97*, 12674−12677.

(23) Marcinek, A.; Leyva, E.; Whitt, D.; Platz, M. S. *J. Am. Chem. Soc.* **1993**, *115*, 8609−8612.

(24) Schnapp, K. A.; Poe, R.; Leyva, E.; Soundarajan, N.; Platz, M. S. *Bioconjugate Chem.* **1993**, *4*, 172−177.

(25) Schnapp, K. A.; Platz, M. S. *Bioconjugate Chem.* **1993**, *4*, 178−183.

(26) Anderson, G. B.; Falvey, D. E. *J. Am. Chem. Soc.* **1993**, *115*, 9870−9871.

(27) Ohana, T; Kaise, M.; Nimura, S.; Kikuchi, O.; Yabe, A. *Chem. Lett.* **1993**, 765−768.

(28) Davidse, P. A.; Kahley, M. J.; McClelland, R. A.; Novak, M. *J. Am. Chem. Soc.* **1994**, *116*, 4513−4514.

(29) Marcinek, A.; Platz, M. S.; Chan, Y. S.; Floresca, R.; Rajagopalan, K.; Golinski, M.; Watt, D. *J. Phys. Chem.* **1994**, *98*, 412−419.

(30) Lamara, K.; Redhouse, A. D.; Smalley, R. K.; Thompson, J. R. *Tetrahedron* **1994**, *50*, 5515−5526.

(31) McClelland, R. A.; Davidse, P. A.; Haczialic, G. *J. Am. Chem. Soc.* **1995**, *117*, 4173−4174.

(32) Robbins, R. J.; Yang, L. L.-N.; Anderson, G. B.; Falvey, D. E. *J. Am. Chem. Soc.* **1995**, *117*, 6544−6552.

(33) Srivastava, S.; Falvey, D. E. *J. Am. Chem. Soc.* **1995**, *117*, 10186−10193.

(34) McClelland, R. A.; Kahley, M. J.; Davidse, P. A. *J. Phys. Org. Chem.* **1996**, *9*, 355−360.

(35) McClelland, R. A.; Kahley, M. J.; Davidse, P. A.; Hadzialic, G. *J. Am. Chem. Soc.* **1996**, *118*, 4794−4803.

(36) Robbins, R. J.; Laman, D. M.; Falvey, D. E. *J. Am. Chem. Soc.* **1996**, *118*, 8127−8135.

(37) Moran, R. J.; Falvey, D. E. *J. Am. Chem. Soc.* **1996**, *118*, 8965−8966.

(38) Morawietz, J.; Sander, W. *J. Org. Chem.* **1996**, *61*, 4351−4354.

(39) Castell, O.; Garcia, V. M.; Bo, C.; Caballol, R. *J. Comput. Chem.* **1996**, *17*, 42−48.

(40) Michalak, J.; Zhai, H. B.; Platz, M. S. *J. Phys. Chem.* **1996**, *100*, 14028−14036.

(41) Sun, X.-Z.; Virrels, I. G.; George, M. W.; Tomioka, H. *Chem. Lett.* **1996**, 1089−1090.

(42) Karney, W. L.; Borden, W. T. *J. Am. Chem. Soc.* **1997**, *119*, 1378−1387.

(43) Karney, W. L.; Borden, W. T. *J. Am. Chem. Soc.* **1997**, *119*, 3347−3350.

(44) Gritsan, N. P.; Yuzawa, T.; Platz, M. S. *J. Am. Chem. Soc.* **1997**, *119*, 5059−5060.

(45) Born, R.; Burda, C.; Senn, P.; Wirz, J. *J. Am. Chem. Soc.* **1997**, *119*, 5061−5062.

(46) Gritsan, N. P.; Zhai, H. B.; Yuzawa, T.; Karweik, D.; Brooke, J.; Platz, M. S. *J. Phys. Chem. A* **1997**, *101*, 2833−2840.

(47) Moran, R. J.; Falvey, D. E. *J. Am. Chem. Soc.* **1996**, *118*, 8965−8966.

(48) Srivastava, S.; Toscano, J. P.; Moran, R. J.; Falvey, D. E. *J. Am. Chem. Soc.* **1997**, *119*, 11552−11553.

(49) Leyva, E.; Sagredo, R. *Tetrahedron* **1998**, *54*, 7367−7374.

(50) Nicolaides, A.; Tomioka, H.; Murata, S. *J. Am. Chem. Soc.* **1998**, *120*, 11530−11531.

(51) Nicolaides, A.; Nakayama, T.; Yamazaki, K.; Tomioka, H.; Koseki, S.; Stracener, L. L.; McMahon, R. J. *J. Am. Chem. Soc.* **1999**, *121*, 10563−10572.

(52) Gritsan, N. P.; Zhu, Z.; Hadad, C. M.; Platz, M. S. *J. Am. Chem. Soc.* **1999**, *121*, 1202−1207.

(53) Gritsan, N. P.; Gudmundsdottir, A. D.; Tigelaar, D.; Platz, M. S. *J. Phys. Chem. A* **1999**, *103*, 3458−3461.

(54) Gritsan, N. P.; Tigelaar, D.; Platz, M. S. *J. Phys. Chem. A* **1999**, *103*, 4465−4469.

(55) Cerro-Lopez, M.; Gritsan, N. P.; Zhu, Z.; Platz, M. S. *J. Phys. Chem. A* **2000**, *104*, 9681−9686.

(56) Srivastava, S.; Ruane, P. H.; Toscano, J. P.; Sullivan, M. B.; Cramer, C. J.; Chiapperino, D.; Reed, E. C.; Falvey, D. E. *J. Am. Chem. Soc.* **2000**, *122*, 8271−8278.

(57) (a) Gritsan, N. P.; Likhotvorik, I.; Tsao, M.-L.; Celebi, N.; Platz, M. S.; Karney, W. L.; Kemnitz, C. R.; Borden, W. T. *J. Am. Chem. Soc.* **2001**, *123*, 1425−1433. (b) Tsao, M.-L.; Gritsan, N.; James, T. R.; Platz, M. S.; Hrovat, D. A.; Borden, W. T. *J. Am. Chem. Soc.* **2003**, *125*, 9343−9358.

(58) Inui, H.; Murata, S. *Chem. Lett.* **2001**, 832−833.

(59) Nicolaides, A.; Enyo, T.; Miura, D.; Tomioka, H. *J. Am. Chem. Soc.* **2001**, *123*, 2628−2636.

(60) (a) Ong, S. Y.; Zhu, P.; Poon, Y. F.; Leung, K.-H.; Fang, W. H. *Chem. Eur. J.* **2002**, *8*, 2163−2171. (b) Ong, S. Y.; Chan, P. Y.; Zhu, P.; Leung, K. H.; Phillips, D. L. *J. Phys. Chem. A* **2003**, *107*, 3858−3865.

(61) (a) Zhu, P.; Ong, S. Y.; Chan, P. Y.; Leung, K. H.; Phillips, D. L. *J. Am. Chem. Soc.* **2001**, *123*, 2645−2649. (b) Zhu, P.; Ong, S. Y.; Chan, P. Y.; Poon, Y. F.; Leung, K. H.; Phillips, D. L. *Chem. Eur. J.* **2001**, *7*, 4928−4936. (c) Chan, P. Y.; Ong, S. Y.; Zhu, P.; Leung, K. H.; Phillips, D. L. *J. Org. Chem.* **2003**, *68*, 5265−5273. (d) Chan, P. Y.; Ong, S. Y.; Zhu, P.; Zhao, C.; Phillips, D. L. *J. Phys. Chem. A* **2003**, *107*, 8067−8074.

(62) Miller, J. A. *Cancer Res.* **1970**, *20*, 559−576.

(63) Scribner, J. D.; Naimy, N. K. *Cancer Res.* **1975**, *35*, 1416−1421.

(64) Miller, E. C. *Cancer Res.* **1978**, *38*, 1479−1496.

(65) Miller, E. C.; Miller, J. A. *Cancer* **1981**, *47*, 2327−2345.

(66) Singer, B.; Kusmierek, J. T. *Annu. Rev. Biochem.* **1982**, *51*, 655−693.

(67) Miller, J. A.; Miller, E. C. *Environ. Health Perspect.* **1983**, *49*, 3−12.

(68) Garner, R. C.; Martin, C. N.; Clayson, D. B. In *Chemical Carcinogens*, 2nd ed.; Searle, C. E., Ed.; ACS Monograph 182; American Chemical Society: Washington, DC, 1984; Vol. 1, pp 175−276.

(69) Famulok, M.; Boche, G. *Angew. Chem., Int. Ed. Engl.* **1989**, *28*, 468−469.

(70) Meier, C.; Boche, G. *Tetrahedron Lett.* **1990**, *31*, 1693−1696.

(71) Humphreys, W. G.; Kadlubar, K. K.; Guengerich, F. P. *Proc. Natl. Acad. Sci. U.S.A.* **1992**, *89*, 8278−8282.

(72) Kadlubar, F. F. In *DNA Adducts of Carcinogenic Amines*; Hemminiki, K., Dipple, A., Shuker, D. E. G., Kadlubar, K. K., Segerbäch, D., Bartsch, H., Eds.; Oxford University Press: Oxford, U.K., 1994; pp 199−216.

(73) Dipple, A. *Carcinogenesis* **1995**, *16*, 437−441.

(74) Novak, M.; Kahley, M. J.; Lin, J.; Kennedy, S. A.; James, T. G. *J. Org. Chem.* **1995**, *60*, 8294−8304.

(75) Cramer, C. J.; Falvey, D. E. *Tetrahedron Lett.* **1997**, *38*, 1515−1518.

(76) Novak, M.; Kennedy, S. A. *J. Am. Chem. Soc.* **1995**, *117*, 574−575.

(77) Hoffman, G. R.; Fuchs, R. P. P. *Chem. Res. Toxicol.* **1997**, *10*, 347−359.

(78) Novak, M.; Kennedy, S. A. *J. Phys. Org. Chem.* **1998**, *11*, 71−76.

(79) Novak, M.; VandeWater, A. J.; Brown, A. J.; Sanzebacher, S. A.; Hunt, L. A.; Kolb, B. A.; Brooks, M. E. *J. Org. Chem.* **1999**, *64*, 6023−6031.

(80) McClelland, R. A.; Ahmad, A.; Dicks, A. P.; Licence, V. *J. Am. Chem. Soc.* **1999**, *121*, 3303−3310.

(81) (a) Sukhai, P.; McClelland, R. A. *J. Chem. Soc., Perkin Trans. 2* **1996**, 1529−1530. (b) Ramllal, P.; McClelland, R. A. *J. Chem. Soc., Perkin Trans. 2* **1999**, 225−232.

(82) Kwok, W. M.; Chan, P. Y.; Phillips, D. L. *J. Phys. Chem. B* **2004**, *108*, 19068−19075.

(83) Chan, P. Y.; Kwok, W. M.; Lam, S. K.; Chiu, P.; Phillips, D. L. *J. Am. Chem. Soc.* **2005**, *127*, 8246−8247.

(84) (a) Brown, B. R.; Yielding, L. W.; White, W. E., Jr. *Mutat. Res.* **1980**, *70*, 17. (b) White, W. E., Jr.; Yielding, L. W. In *Methods in Enzymology Vol. XLVI Affinity Labeling*; Jakoby, W. B., Wilchek, M., Eds.; Academic Press, Inc.: Orlando, FL, 1977; pp 646−647. (c) Wheeler, O. H.; Gonzalez, D. *Tetrahedron* **1964**, *20*, 189.

(85) (a) Li, Y.-L.; Leung, K. H.; Phillips, D. L. *J. Phys. Chem. A* **2001**, *105*, 10621−10625. (b) Li, Y.-L.; Chen, D.-M.; Wang, D.; Phillips, D. L. *J. Org. Chem.* **2002**, *67*, 4228−4235. (c) Li, Y.-L.; Wang, D.; Phillips, D. L. *J. Chem. Phys.* **2002**, *117*, 7931−7941.

(86) Frisch, M. J.; Trucks, G. W.; Schlegel, H. B.; Scuseria, G. E.; Robb, M. A.; Cheeseman, J. R.; Zakrzewski, V. G.; Montgomery, J. A., Jr.; Stratmann, R. E.; Burant, J. C.; Dapprich, S.; Millam, J. M.; Daniels, A. D.; Kudin, K. N.; Strain, M. C.; Farkas, O.; Tomasi, J.; Barone, V.; Cossi, M.; Cammi, R.; Mennucci, B.; Pomelli, C.; Adamo, C.; Clifford, S.; Ochterski, J.; Petersson, G. A.; Ayala, P. Y.; Cui, Q.; Morokuma, K.; Malick, D. K.; Rabuck, A. D.; Raghavachari, K.; Foresman, J. B.; Cioslowski, J.; Ortiz, J. V.; Baboul, A. G.; Stefanov, B. B.; Liu, G.; Liashenko, A.; Piskorz, P.; Komaromi, I.; Gomperts, R.; Martin, R. L.; Fox, D. J.; Keith, T.; Al-Laham, M. A.; Peng, C. Y.; Nanayakkara, A.; Gonzalez, C.; Challacombe, M.; Gill, P. M. W.; Johnson, B.; Chen, W.; Wong, M. W.; Andres, J. L.; Gonzalez, C.; Head-Gordon, M.; Replogle, E. S.; Pople, J. A. *Gaussian A.7*; Gaussian, Inc.: Pittsburgh, PA, 1998.

(87) McClelland, R. A.; Gadsoy, T. A.; Ren, D. *Can. J. Chem.* **1998**, *76*, 1327.

(88) McDonald, R. N.; Chowdhury, A. K. *J. Am. Chem. Soc.* **1980**, *102*, 5119−5120.

(89) Kung, A. C.; McIlroy, S. P.; Falvey, D. E. *J. Org. Chem.* **2005**, *70*, 5283−5290.